

# Effect of Material Thickness and Coffee Thermocycling on the Color Stability and Translucency of Additively and Subtractively Manufactured Resin-Based Materials for Definitive Restorations

Deniz Yılmaz, DDS, PhD

Department of Prosthodontics, Faculty of Dentistry, Alanya Alaaddin Keykubat University, Istanbul, Turkey.

Gabriela Panca Sabatini, DDS, MSc

Department of Prosthodontics, University of São Paulo, São Paulo, Brazil.

Çiğdem Kahveci, DDS, PhD

Ordu Oral and Dental Health Center, Ordu, Turkey.

Hyung-In Yoon, DDS, MSD, PhD

Department of Prosthodontics, School of Dentistry and Dental Research Institute, Seoul National University, Seoul, Republic of Korea; Department of Reconstructive Dentistry and Gerodontology, School of Dental Medicine, University of Bern, Bern, Switzerland.

Burak Yılmaz, DDS, PhD

Department of Reconstructive Dentistry and Gerodontology and Department of Restorative, Preventive and Pediatric Dentistry, School of Dental Medicine, University of Bern, Bern, Switzerland; Division of Restorative and Prosthetic Dentistry, The Ohio State University College of Dentistry, Columbus, Ohio, USA.

Gülce Çakmak, DDS, PhD

Department of Reconstructive Dentistry and Gerodontology, School of Dental Medicine, University of Bern, Bern, Switzerland.

Mustafa Borga Dönmez, DDS, PhD

Department of Prosthodontics, Faculty of Dentistry, Istinye University, Istanbul, Turkey; Department of Reconstructive Dentistry and Gerodontology, School of Dental Medicine, University of Bern, Bern, Switzerland.

**Purpose:** To evaluate the effect of material thickness and coffee thermocycling on the optical properties of definitive resin-based materials created via additive manufacturing (AM) and subtractive manufacturing (SM). **Materials and Methods:** Specimens were prepared in three thicknesses (1, 1.5, and 2 mm) from three AM (3D-CB, 3D-TH, and 3D-CT) and two SM (G-CAM and VE) resin-based materials (n = 15 per material and thickness combination). Color coordinates of each specimen were measured after polishing and after 10,000 cycles of coffee thermocycling. Color differences ( $\Delta E_{00}$ s) and relative translucency parameter (RTP) values were calculated. After logarithmic transformation,  $\Delta E_{00}$  values were analyzed with two-way ANOVA, while RTP values were analyzed with generalized linear model test ( $\alpha = .05$ ). **Results:** 3D-TH had the highest pooled  $\Delta E_{00}$  and G-CAM had the lowest ( $P \leq .004$ ). 3D-CB had higher pooled  $\Delta E_{00}$  than VE and 3D-CT ( $P \leq .002$ ). For the SM group, the 1.5-mm and 2-mm 3D-CT specimens and 1-mm 3D-TH specimens had lower  $\Delta E_{00}$  than 1.5-mm and 2-mm 3D-TH specimens ( $P \leq .036$ ). Most of the AM specimens and 1-mm VE specimens had higher  $\Delta E_{00}$  than 2-mm G-CAM specimens ( $P \leq .029$ ). Further, most AM specimens had higher  $\Delta E_{00}$  than 1.5-mm G-CAM specimens ( $P \leq .006$ ). RTP values increased in order of 3D-CT, G-CAM, VE, 3D-CB, and 3D-TH specimens ( $P < .001$ ). Increased thickness and coffee thermocycling mostly reduced RTP ( $P < .001$ ). **Conclusions:** 3D-TH typically had higher color change values than SM specimens, while G-CAM typically had lower color change values than AM specimens. Only the 1.5-mm and 2-mm 3D-TH specimens had unacceptable color changes. Thickness and coffee thermocycling mostly reduced the translucency. *Int J Prosthodont* 2024;37(suppl):s143–s150. doi: 10.11607/ijp.8870

Correspondence to:  
Dr Mustafa Borga Dönmez,  
mustafa-borga.doenmez@unibe.ch

Submitted September 28, 2023;  
accepted November 15, 2023.

©2024 by Quintessence  
Publishing Co Inc.

Advancements in CAD/CAM technologies have facilitated the use of additive<sup>1,2</sup> and subtractive manufacturing.<sup>3</sup> Additive manufacturing (AM) enables the fabrication of products with complex geometries due to its layer-by-layer construction model with relatively lower amounts of excess material when compared to subtractive manufacturing (SM).<sup>4</sup> A wide range of materials for different indications are available with AM<sup>3,5</sup>; of those, some composite resin materials are indicated for definitive prostheses.<sup>6,7</sup> Recent studies have shown that AM composite resins have similar fabrication trueness<sup>6,8</sup> and mechanical properties<sup>9,10</sup> to those SM resins with similar chemical compositions. In addition, urethane-based resins are also available for the AM of definitive prostheses.<sup>11,12</sup>

SM has been the dominant fabrication method for CAD/CAM restorations with resin-based materials due to the standardized polymerized conditions in the form of millable blocks or disks.<sup>13</sup> To improve the mechanical properties of resin materials, nanotechnology has been incorporated into the fabrication of these prepolymerized resin-based CAD/CAM materials.<sup>14</sup> A nanographene-reinforced polymethylmethacrylate (PMMA) was recently introduced, indicated for fabricating definitive prostheses.<sup>6,15</sup> Graphene particles have a unique arrangement of carbon atoms, which have a honeycomb shape<sup>16</sup> and may improve the mechanical properties of dental PMMA materials.<sup>17</sup> However, various properties of nanographene-reinforced PMMA should be further investigated for clinical implementation.

Translucency is a critical parameter to consider when choosing a material for tooth restoration in the esthetic zone.<sup>18,19</sup> Material thickness and chemical composition are among the factors that affect the translucency of a restorative material.<sup>20,21</sup> Moreover, translucency is not the only optical parameter that affects longevity, as color stability of a definitive prosthesis might also determine its clinical service time.<sup>22</sup> A definitive restorative material must be resistant to discoloration caused by temperature changes in the oral cavity and discolorants while maintaining its original shade with long-term color stability.<sup>21</sup> The mechanical properties of AM composite resins<sup>3,7,10,23–26</sup> and nanographene-reinforced PMMA<sup>6,14,17,27–30</sup> have previously been investigated. However, the number of studies on their optical properties is scarce<sup>2,13,29,31,32</sup>; even though these studies have reported acceptable color stability after coffee thermocycling<sup>13</sup> and similar translucency to that of lithium disilicate,<sup>29</sup> none have investigated the combined effect of material thickness and coffee thermocycling on the optical properties of these materials. Therefore, the present study aimed to evaluate the color stability and translucency of two polyurethane acrylate resins and a definitive composite resin for AM, and a nanographene-reinforced PMMA and a polymer-infiltrated ceramic network for SM in different

thicknesses (1, 1.5, and 2 mm) when subjected to coffee thermocycling. The null hypotheses were that (1) material type and thickness would not affect the color stability and (2) material type, thickness, and coffee thermocycling would not affect the translucency.

## MATERIALS AND METHODS

A total of 225 rectangular specimens were fabricated in three thicknesses (1, 1.5, and 2 mm) from five different restorative materials in shade A1: two urethane acrylate resins for AM (C&B Permanent, ODS [3D-CB]; and Tera Harz TC-80DP, Graphy [3D-TH]); a composite resin for AM (Crowntec, Saremco Dental [3D-CT]); a nanographene-reinforced PMMA for SM (G-CAM, Graphenano Dental [G-CAM]); and a polymer-infiltrated ceramic network for SM (Vita Enamic, Vita Zahnfabrik [VE]). Fifteen specimens were created per thickness and material combination (Table 1). To fabricate SM specimens, a rectangular prism (10 × 10 × 16 mm) was designed in standard tessellation language (STL) format with a design software program (Meshmixer version 3.5.474, Autodesk). This STL file was used to mill (PrograMill PM7, Ivoclar Vivadent) prisms from G-CAM disks, which were then wet-sliced with the same precision cutter to obtain specimens in final thicknesses (1, 1.5, or 2 mm). The VE specimens were prepared by sectioning CAD/CAM blocks in desired thickness with a precision cutter (Vari/Cut VC-50, Leco). To fabricate AM specimens, three STL files with rectangular designs (10 × 10 × 1.0 mm, 10 × 10 × 1.5 mm, and 10 × 10 × 2.0 mm) were made using the same design software program. Each STL file was imported separately into a nesting software program (Composer, Asiga) and positioned parallel to the build platform. Support structures were generated automatically, and this standardized configuration was duplicated 15 times for each material. The specimens were printed using a digital light processing (DLP)-based 3D printer (MAX UV, Asiga) with a layer thickness of 50 μm. After printing and a 10-minute drip time, specimens were removed from the build platform, and the support structures were cut off with a side cutter. The 3D-TH and 3D-CB specimens were cleaned ultrasonically (Ultracleaner 07-08, Eltrosonic) in 96% ethanol (Ethanol absolut, Grogg Chemie) for 45 seconds before being thoroughly cleaned with an ethanol-soaked cloth. 3D-CT specimens were cleaned using only an ethanol-soaked cloth. Specimens were air-dried and postpolymerized with 4,000 flashes of light exposure (2,000 flashes for each side; 5-minute cool-down between sets) using a xenon lamp-polymerization unit (Otoflash G171, NK Optik) under nitrogen oxide gas atmosphere.

After postpolymerization, remaining support structures were removed using ×3.5 magnification loupes (EyeMag Pro, Zeiss). One test surface of each specimen

**Table 1** Details of the Resin-Based Materials Tested

Material (product name)	Chemical Composition	Abbreviation	Manufacturer
Urethane acrylate resin for AM (C&B Permanent)	Diurethane dimethacrylate, 2-propenoic acid, 2-methyl-, (1-methylethylidene) bis (4,1-phenyleneoxy(1-methyl-2,1-ethanediyl)) ester, 2-hydroxyethyl methacrylate, diphenyl (2,4,6-trimethylbenzoyl) phosphine oxide, and additives	3D-CB	ODS
Composite resin for AM (Crowntec)	Up to 50% in weight, 0.7-mm barium aluminum borosilicate glass fillers, 4,4'-isopropylidiphenol, ethoxylated and 2-methylprop-2-enoic acid, silanized dental glass, pyrogenic silica, catalysts, inhibitors	3D-CT	Saremco Dental
Urethane acrylate resin for AM (TC-80DP)	Urethane acrylate oligomer, bisphenol A ethoxylate dimethacrylate, 2-hydroxyethyl methacrylate, diphenyl (2,4,6-trimethylbenzoyl) phosphine oxide, and additives	3D-TH	Graphy
Nanographene-reinforced polymethylmethacrylate for SM (G-CAM)	Not disclosed	G-CAM	Graphenano Dental
Polymer-infiltrated ceramic network for SM (Vita Enamic)	14 wt% methacrylate polymer (urethane dimethacrylate and triethylene glycol dimethacrylate) and 86 wt% fine-structure feldspar ceramic network	VE	Vita Zahnfabrik

**Table 2** Polishing Procedures of the Tested Materials

Material	Polishing procedure
3D-CB	Composite diamond-polishing kit (Diatech, Coltène)
3D-CT	Polishing with yellow-composite polishing instrument for 90 s at 5,000 rpm
3D-TH	Finishing with a polishing paste (Zircon Brite, Dental Ventures of America) and wool felt polishing wheels for 120 s at 5,000 rpm
G-CAM	Polishing with pumice slurry (Pumice fine, Benco Dental) for 90 s at 1,500 rpm Finishing with a polishing paste (Fabulustre, Grobet USA) for 90 s
VE	Manufacturer's proprietary polishing set (Enamic Polishing Set Clinical, Vita Zahnfabrik) Prepolishing with diamond-coated pink instruments for 30 s at 9,000 rpm, followed by high-gloss polishing with diamond-coated gray instruments for 30 s at 6,000 rpm Finishing with a polishing paste (Zircon Brite) and wool felt polishing wheels for 90 s at 5,000 rpm

was initially polished with silicon carbide papers (280, 360, and 1,000 grit) using a polishing machine (LaboPol, Struers) for 15 seconds. The treated surfaces were further polished according to the manufacturers' instructions (Table 2). A digital caliper (NB60, Mitutoyo America) was used to ensure the final thickness (1, 1.5, and  $2 \pm 0.03$  mm) of each specimen. The specimens were ultrasonically cleaned in distilled water for 10 minutes and dried gently after polishing.

Initial color coordinate measurements ( $L^*$ ,  $a^*$ , and  $b^*$ ) of specimens were performed in a room with daylight over gray, white, and black backgrounds using a digital spectrophotometer (CM-26d, Konica Minolta) with an integrated Commission International de l'Eclairage (CIE) D65 illuminant and uses the CIE Standard (2-degree) human observer characteristics.<sup>13</sup> The spectrophotometer was calibrated before measuring each specimen set, and saturated sucrose solution was used to ensure optical contact between the specimen and the background. A single operator (G.P.S.) performed three measurements on each background for each specimen, and these values were averaged. Specimens were then subjected to 10,000 cycles of thermal aging (5° to 55°C; 30-second

dwelt time; 10-second transfer time; Thermocycler, SD Mechatronik) in a coffee solution. The coffee solution was freshly prepared every 12 hours with a ratio of one tablespoon of coffee (Intenso Roasted and Ground Coffee, Kaffeehof) to 177 mL of water.<sup>20</sup> The coffee extracts were cleansed by brushing the specimens 10 times with a toothpaste (Nevadent Complex 3, DENTAL-Kosmetik). Then, the specimens were ultrasonically cleaned for 10 minutes and dried. After coffee thermocycling, color coordinate measurements were repeated with the same methods mentioned above. The color difference ( $\Delta E_{00}$ ) values were calculated using the coordinates measured on the gray background and the following CIEDE2000 color difference formula, with parametric factors set to 120:

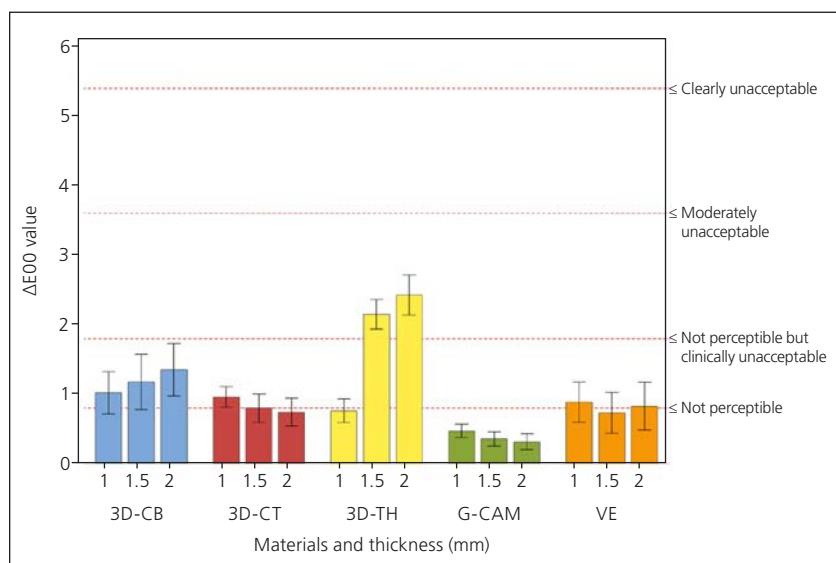
$$\text{CIEDE2000} = [(\Delta L'/kLSL)^2 + (\Delta C'/kCSC)^2 + (\Delta H'/kHSH)^2 + RT(\Delta C'/kCSC)(\Delta H'/kHSH)]^{1/2}$$

The relative translucency parameter (RTP) value of each specimen before and after coffee thermocycling was calculated using the coordinates measured on white and black backgrounds with the same formula.

**Table 3**  $\Delta E_{00}$  Values

	3D-CB	3D-CT	3D-TH	G-CAM	VE
<b>1-mm specimens</b>					
After log conversion	$0 \pm 0.2^{CDE}$	$0 \pm 0.1^{CD}$	$-0.2 \pm 0.2^{BC}$	$-0.4 \pm 0.2^{AB}$	$-0.1 \pm 0.2^{BC}$
Raw data	$1.0 \pm 0.6$	$1.0 \pm 0.3$	$0.8 \pm 0.3$	$0.5 \pm 0.2$	$0.9 \pm 0.5$
<b>1.5-mm specimens</b>					
After log conversion	$0 \pm 0.4^{CDE}$	$-0.1 \pm 0.2^{BCD}$	$0.3 \pm 0.1^E$	$-0.5 \pm 0.3^{AB}$	$-0.2 \pm 0.3^{ABCD}$
Raw data	$1.2 \pm 0.7$	$0.8 \pm 0.4$	$2.2 \pm 0.4$	$0.4 \pm 0.2$	$0.7 \pm 0.5$
<b>2-mm specimens</b>					
After log conversion	$0.1 \pm 0.2^{DE}$	$-0.2 \pm 0.2^{ABCD}$	$0.4 \pm 0.1^E$	$-0.6 \pm 0.3^A$	$-0.2 \pm 0.4^{ABCD}$
Raw data	$1.4 \pm 0.7$	$0.7 \pm 0.4$	$2.4 \pm 0.5$	$0.3 \pm 0.2$	$0.8 \pm 0.6$
<b>Total</b>					
After log conversion	$0 \pm 0.3^c$	$-0.1 \pm 0.2^b$	$0.2 \pm 0.3^d$	$-0.5 \pm 0.3^a$	$-0.2 \pm 0.3^b$
Raw data	$1.2 \pm 0.7$	$0.8 \pm 0.3$	$1.8 \pm 0.8$	$0.4 \pm 0.2$	$0.8 \pm 0.5$

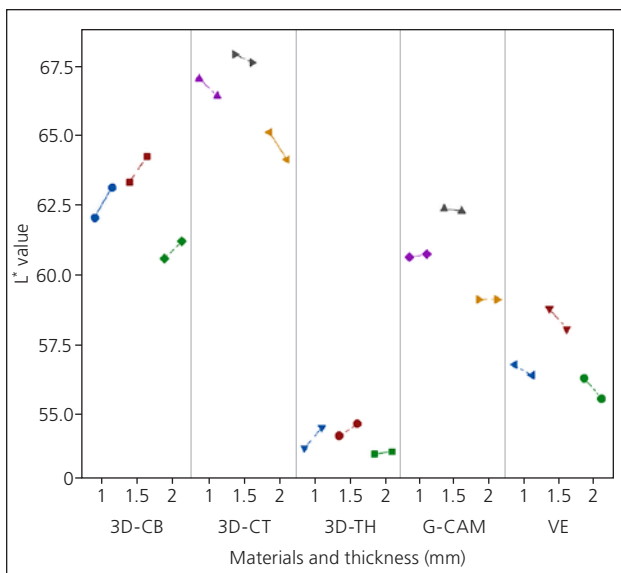
Different superscript uppercase and lowercase letters indicate significant differences among material-thickness pairs and among materials, respectively. Total values are derived from the pooled data of each thickness within each material ( $P < .05$ ).

**Fig 1** Box-plot graph of raw  $\Delta E_{00}$  values of each material-thickness pair.

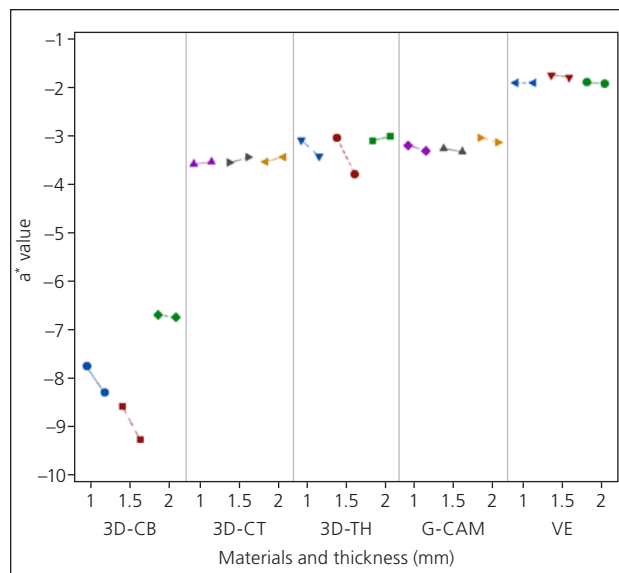
## RESULTS

Table 3 summarizes the descriptive statistics of log-transformed and raw  $\Delta E_{00}$  values for all materials. In terms of the effect on  $\Delta E_{00}$  values, the interaction between the material type and thickness was significant, as well as the effect of material type ( $P < .001$ ). The  $\Delta E_{00}$  value was the highest in the 3D-TH group ( $P \leq .004$ ) and lowest in the G-CAM group ( $P < .001$ ). In addition, the VE and 3D-CT groups had similar  $\Delta E_{00}$  values ( $P > .050$ ), which were lower than that of the 3D-CB group ( $P \leq .002$ ). Considering the interaction between the material type and thickness, 1.5-mm and 2-mm 3D-TH specimens had higher  $\Delta E_{00}$  values than 1-mm 3D-TH specimens, 3D-CT specimens of the same thicknesses, and all SM specimens ( $P \leq .036$ ). The 2-mm G-CAM specimens had lower  $\Delta E_{00}$  than the 1-mm VE and all AM specimens ( $P \leq .029$ ), except 2-mm 3D-CT specimens ( $P = .050$ ). Other than the 1-mm 3D-TH and 1.5-mm and 2-mm 3D-CT specimens ( $P \geq .213$ ), 1.5-mm G-CAM specimens had lower  $\Delta E_{00}$  than tested AM materials ( $P \leq .006$ ). Figure 1 shows the raw  $\Delta E_{00}$  values of each material-thickness pair. Figures 2 to 4 show

Normality of data was evaluated using Kolmogorov Smirnov tests, which yielded normal distribution for both  $\Delta E_{00}$  and RTP data after logarithmic transformation. The log-transformed  $\Delta E_{00}$  data was evaluated using two-way ANOVA and post-hoc Scheffe tests, considering material type and thickness as main effects and including their interaction. The log-transformed RTP data was assessed using a generalized linear model test with material type, thickness, and aging (coffee thermocycling) as main effects, and their interactions were included.  $\Delta E_{00}$  values were further evaluated using the previously set thresholds (not perceptible:  $\leq 0.8$ ; perceptible but clinically acceptable:  $\leq 1.8$ ; moderately unacceptable:  $\leq 3.6$ ; clearly unacceptable:  $\leq 5.4$ ; and extremely unacceptable:  $> 5.4$  units) by Paravina et al.<sup>33</sup> The RTP change ( $\Delta RTP$ ) caused by coffee thermocycling was evaluated using the previously set thresholds (perceptibility = 0.62 units; acceptability = 2.62 units) by Salas et al.<sup>34</sup>



**Fig 2** Trend of L\* color coordinate change within each material-thickness pair before and after thermocycling.



**Fig 3** Trend of a\* color coordinate change within each material-thickness pair before and after thermocycling.

how color coordinates change after coffee thermocycling within each material-thickness pair.

Descriptive statistics of log-transformed and raw RTP values of each material-thickness pair are presented in Table 4. The main effect of each factor (material type, thickness, and aging) and their interactions significantly affected the RTP ( $P < .001$ ), except for the interaction among all main factors ( $P = .110$ ) and the interaction between thickness and aging ( $P = .930$ ). Regardless of the thickness, the RTP of materials were significantly different from each other ( $P < .001$ ), with the increasing order of 3D-CT, G-CAM, VE, 3D-CB, and 3D-TH. Regardless of the material, the RTP values significantly reduced as specimen thickness increased ( $P < .001$ ). Aging by coffee thermocycling significantly increased the RTP of all materials ( $P < .001$ ) except for 3D-CT and VE specimens ( $P \geq .380$ ). Figure 5 shows the raw RTP values of each material-thickness pair under different aging conditions.

## DISCUSSION

Significant differences were observed among the  $\Delta E_{00}$  values of tested material-thickness pairs. Therefore, the first null hypothesis was rejected. When  $\Delta E_{00}$  values were further evaluated according to the previously set threshold values,<sup>33</sup> only the 1.5-mm and 2-mm 3D-TH specimens had moderately unacceptable color changes ( $\Delta E_{00} \geq 2.2$ ). 3D-TH specimens also had the highest  $\Delta E_{00}$  values among tested materials within these thicknesses, except for 3D-CB. Change in color coordinates may be attributed to this difference because, regardless of the thickness and condition, 3D-TH specimens had

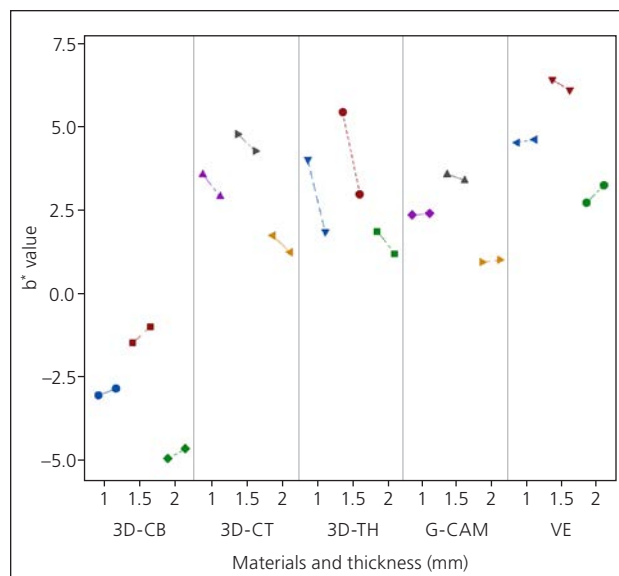


**Fig 4** Trend of b\* color coordinate change within each material-thickness pair before and after thermocycling.

lower L\* values, which indicates lower lightness, and had higher b\* values after coffee thermocycling, which indicates a more blueish color. It should also be noted that 1-mm 3D-TH specimens had a mean  $\Delta E_{00}$  value of 0.8, which is marginally imperceptible, and a pooled mean  $\Delta E_{00}$  value of 1.8, which is perceptible but clinically acceptable. Among the remaining material-thickness pairs, G-CAM and 1.5-and 2-mm 3D-CT and VE specimens had imperceptible color change after coffee thermocycling ( $\Delta E_{00} \leq 0.8$ ), while other pairs had perceptible color change, with the highest mean  $\Delta E_{00}$  value of 1.4.

**Table 4** Mean RTP Values After Log Conversion of Raw Data

	Thickness	Coffee thermocycling			
		Before		After	
		After log conversion	Raw data	After log conversion	Raw data
3D-CB	1 mm	1.5 ± 0 <sup>CD*</sup>	29.4 ± 1.1	1.5 ± 0 <sup>CD^</sup>	31.4 ± 0.6
	1.5 mm	1.3 ± 0 <sup>BD*</sup>	20.9 ± 0.9	1.4 ± 0 <sup>BD^</sup>	23.1 ± 0.4
	2 mm	1.2 ± 0 <sup>AD*</sup>	14.9 ± 0.6	1.2 ± 0 <sup>AD^</sup>	16.7 ± 0.4
3D-CT	1 mm	1.3 ± 0 <sup>CA</sup>	20.9 ± 0.4	1.3 ± 0 <sup>CA</sup>	21.1 ± 0.4
	1.5 mm	1.2 ± 0 <sup>bA</sup>	14.5 ± 0.4	1.2 ± 0 <sup>bA</sup>	14.3 ± 0.3
	2 mm	1 ± 0 <sup>aA</sup>	10 ± 0.2	1 ± 0 <sup>aA</sup>	9.8 ± 0.3
3D-TH	1 mm	1.4 ± 0 <sup>CE*</sup>	32.2 ± 0.9	1.3 ± 0 <sup>CE^</sup>	34 ± 0.8
	1.5 mm	1.2 ± 0 <sup>bE*</sup>	24.8 ± 0.5	1.2 ± 0 <sup>bE^</sup>	25.8 ± 0.6
	2 mm	1.4 ± 0.1 <sup>aE*</sup>	18.6 ± 0.8	1.3 ± 0.1 <sup>aE^</sup>	19.7 ± 0.6
G-CAM	1 mm	1.4 ± 0 <sup>CB*</sup>	25 ± 0.6	1.4 ± 0 <sup>CB^</sup>	25.7 ± 1.1
	1.5 mm	1.2 ± 0 <sup>BB*</sup>	17.6 ± 0.6	1.3 ± 0 <sup>BB^</sup>	18.3 ± 0.7
	2 mm	1.1 ± 0 <sup>aB*</sup>	12 ± 0.4	1.1 ± 0 <sup>aB^</sup>	12.5 ± 0.3
VE	1 mm	1.5 ± 0 <sup>C</sup>	28.9 ± 1.3	1.5 ± 0 <sup>C</sup>	29.5 ± 1.2
	1.5 mm	1.3 ± 0 <sup>bC</sup>	20.9 ± 1.2	1.3 ± 0 <sup>bC</sup>	21.2 ± 1.5
	2 mm	1.2 ± 0 <sup>aC</sup>	14.8 ± 1.2	1.2 ± 0 <sup>aC</sup>	14.7 ± 1.2

Different superscript lowercase letters indicate significant differences among different thicknesses within each material–time interval pair. Different superscript uppercase letters indicate significant differences among tested materials within each thickness–time interval pair. Different symbols indicate significant differences between time intervals within each material–thickness pair ( $P < .05$ ). Data are presented as mean ± SD.

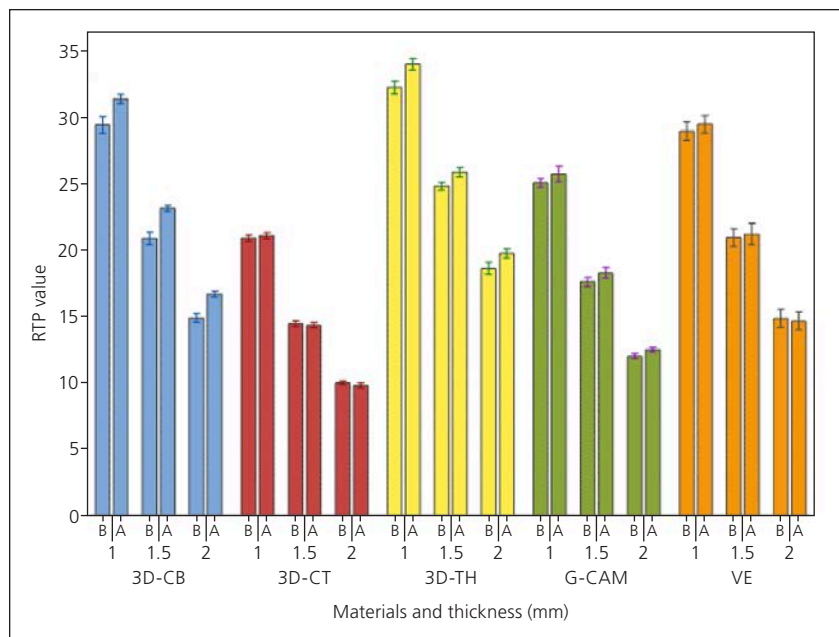


**Fig 5** Raw RTP values of each material–thickness pair before (B) and after (A) thermocycling.

In addition, increased thickness did not affect the  $\Delta E_{00}$  values within each material, other than 3D-TH. Considering these findings, it can be stated that 3D-TH was the most susceptible to discoloration among tested materials; yet, tested materials may be considered promising in terms of color stability given

the duration of coffee thermocycling that could be considered excessive in actual clinical situations.

Regardless of the thickness, G-CAM had imperceptible color change and either significantly or nonsignificantly lower  $\Delta E_{00}$  values than the other materials. A similar trend was also observed for VE, even though the 1-mm specimens had marginally perceptible color change (mean  $\Delta E_{00} = 0.9$ ). The fabrication process of G-CAM and VE may be related to these findings, as they were the only SM materials tested in the present study and are polymerized under standardized conditions that involve high temperature and pressure.<sup>13</sup> Water absorption leads to the deterioration of polymeric chains in resin-based materials.<sup>17</sup> However, considering that VE comprises a high ratio of feldspar ceramic network and the fact that G-CAM had nonsignificantly lower  $\Delta E_{00}$  values than VE, it can be speculated that the addition of graphene increased the discoloration resistance of G-CAM. This interpretation is in



line with the results of Çakmak et al,<sup>13</sup> as the authors have also reported imperceptible color change and nonsignificantly lower  $\Delta E_{00}$  values for G-CAM when compared with PMMA after coffee thermocycling. Nevertheless, a study based on the chemical composition of G-CAM is necessary to substantiate this hypothesis, as the manufacturer of G-CAM has not disclosed its composition.

Tested AM composite resins were relatively more susceptible to discoloration, which could be attributed to the nature of this manufacturing method. Considering that AM is based on the accumulation of consecutive layers, which are polymerized one at a time, residual monomers and microporosities caused by incomplete polymerization might have led to higher  $\Delta E_{00}$  values.<sup>2</sup> While the differences among the tested AM composite resins were nonsignificant within 1-mm specimens, 3D-CT specimens had either significantly or nonsignificantly lower  $\Delta E_{00}$  values as the thickness increased. Resin viscosity is affected by a wide range of factors related to its chemical composition.<sup>5</sup> The 3D-CB viscosity was lower than that of 3D-TH and 3D-CT, which were within the same range (80 mPa\*s for 3D-CB; 2,800 mPa\*s for 3D-TH; and 2.500 to 6.000 mPa\*s for 3D-CT).<sup>35–37</sup> Higher viscosity might have deteriorated the printing process and layer unification of 3D-TH when compared with 3D-CB, while the chemical differences between 3D-CT and other AM composite resins may be associated with 3D-CT's nonsignificantly lower  $\Delta E_{00}$  values. However, the authors are unaware of any studies on the color stability of tested AM composite resins; thus, comparisons with previous studies were not possible.

The hydroxyl groups in the resin structure can form hydrogen bonds with water molecules; consequently, the proportion of each monomer in the resin determines its water absorption capacity. Due to the absence of hydroxyl groups in the structure of bisphenol A ethoxylated dimethacrylate (Bis-EMA), resins containing a high proportion of this monomer exhibited reduced water absorption.<sup>38</sup> The 3D-CT and 3D-TH materials used in the present study comprise hydrophobic Bis-EMA, while the 3D-CB material consists of diurethane dimethacrylate oligomers. Although the main chemical composition of 3D-TH and 3D-CB materials are urethane acrylate-based, 3D-CT is a glassfiller-reinforced composite resin for 3D printing. 3D-TH and 3D-CB materials had greater and more perceptible color change than 3D-CT, possibly due to the differences in chemical composition, including the particle size and distribution, polarity of monomers, amount of cross-linking, initiator system, and pigment stability.

Tested material-thickness pairs had different RTP values before and after coffee thermocycling. In addition, coffee thermocycling increased the RTP values of 3D-CB, 3D-TH, and G-CAM. Therefore, the second null hypothesis was also rejected. Regardless of the condition, the RTP values of materials were increased in the following order: 3D-CT,

G-CAM, VE, 3D-CB, and 3D-TH. When the  $\Delta RTP$  values were evaluated according to set thresholds,<sup>34</sup> 3D-CB and VE specimens had imperceptible changes ( $\Delta RTP \leq 0.5$ ) and 2-mm 3D-CT and G-CAM specimens had acceptable changes ( $\Delta RTP = 2$ ) before coffee thermocycling. After coffee thermocycling, the differences between 3D-CB and VE ( $\Delta RTP \leq 2$ ), 1-mm 3D-CB and 3D-TH ( $\Delta RTP = 2.6$ ), and 2-mm G-CAM and VE ( $\Delta RTP = 2.2$ ) specimens were acceptable. Increased thickness not only significantly reduced the RTP values but also led to unacceptable changes ( $\Delta RTP \geq 4.5$ ), regardless of the material and condition. Even though coffee thermocycling increased the RTP values of 3D-CB, 3D-TH, and G-CAM for each tested thickness, this effect was either imperceptible or clinically acceptable ( $\Delta RTP \leq 2.2$ ).

Although this study was the first on the translucency of tested AM composite resins, recent studies have focused on the translucency of other AM composite resins indicated for definitive restorations.<sup>31,32</sup> One of those studies concluded that the tested AM resin had a greater translucency than some of the tested SM composites,<sup>31</sup> while the other study showed that printing orientation affected the translucency depending on the resin shade.<sup>32</sup> In addition, Agarwalla et al compared the translucency VE and G-CAM<sup>29</sup> and concluded that 1-mm G-CAM and VE specimens had similar translucency values, which contradicts the results of the present study. However, it should be noted that a different formula was used to calculate translucency values in the other study.<sup>29</sup>

Even though significant differences were observed among tested material-thickness pairs, absence of a power analysis was one of the limitations of the present study. In addition, the methodology of coffee thermocycling could not simulate intraoral conditions to its full extent given that saliva was not included and coffee was the only discolorant. It should also be emphasized that coffee thermocycling led to discoloration of both polished and unpolished specimen surfaces, and this might have aggravated discoloration. Even though AM composite resins indicated for definitive restorations are relatively new, the fact that only five CAD/CAM materials of a single shade were tested was another limitation. Also, all AM specimens were printed with a single 3D printer. Future studies should investigate the optical and mechanical properties of tested materials when subjected to other discolorants, brushing, and cyclic loading to broaden the knowledge on their applicability.

## CONCLUSIONS

Within the limitations of this *in vitro* study, the following conclusions can be drawn:

1. Increased thickness only affected the color change of 3D-TH groups, as the 1-mm specimens had lower



- values than those of other thicknesses. In addition, of the 1.5-mm and 2-mm specimens, 3D-TH showed greater color changes than SM specimens.
- When reported thresholds were considered, only 1.5-mm and 2-mm 3D-TH specimens had unacceptable color change after coffee thermocycling.
  - G-CAM mostly had lower color changes than AM specimens.
  - Increased thickness led to significantly reduced translucency for all materials.
  - Coffee thermocycling reduced the translucency of all materials except 3D-CT and VE.

## ACKNOWLEDGMENTS

The authors report no conflicts of interest.

## REFERENCES

- Atria PJ, Bordin D, Marti F, et al. 3D-printed resins for provisional dental restorations: Comparison of mechanical and biological properties. *J Esthet Restor Dent* 2022;34:804–815.
- Alharbi N, Alharbi A, Osman R. Stain susceptibility of 3D-printed nanohybrid composite restorative material and the efficacy of different stain removal techniques: An in vitro study. *Materials (Basel)* 2021;14:5621.
- Grzebieluch W, Kowalewski P, Grygier D, Rutkowska-Gorczyca M, Kozakiewicz M, Jurczynski K. Printable and machinable dental restorative composites for CAD/CAM application-comparison of mechanical properties, fractographic, texture and fractal dimension analysis. *Materials (Basel)* 2021;14:4919.
- Jockusch J, Özcan M. Additive manufacturing of dental polymers: An overview on processes, materials and applications. *Dent Mater J* 2020:2019–2123.
- Vyas A, Garg V, Ghosh SB, Bandyopadhyay-Ghosh S. Photopolymerizable resin-based 3D printed biomedical composites: Factors affecting resin viscosity. *Mater Today Proc* 2022;62:1435–1439.
- Çakmak G, Rusa AM, Donmez MB, et al. Trueness of crowns fabricated by using additively and subtractively manufactured resin-based CAD-CAM materials. *J Prosthet Dent* 2022:S0022-3913(22)00690-4.
- Donmez MB, Çakmak G, Yılmaz D, et al. Bond strength of additively manufactured composite resins to dentin and titanium when bonded with dual-polymerizing resin cements. *J Prosthet Dent* 2023. Epub ahead of print.
- Demirel M, Diken Türksayar AA, Donmez MB. Fabrication trueness and internal fit of hybrid abutment crowns fabricated by using additively and subtractively manufactured resins. *J Dent* 2023;136:104621.
- Diken Türksayar AA, Demirel M, Donmez MB, Olcay EO, Eyüboğlu TF, Özcan M. Comparison of wear and fracture resistance of additively and subtractively manufactured screw-retained, implant-supported crowns. *J Prosthet Dent* 2023:S0022-3913(23)00418-3.
- Donmez MB, Okutan Y. Marginal gap and fracture resistance of implant-supported 3D-printed definitive composite crowns: An in vitro study. *J Dent* 2022;124:104216.
- Nam NE, Hwangbo NK, Kim JE. Effects of surface glazing on the mechanical and biological properties of 3D printed permanent dental resin materials. *J Prosthodont Res* 2023. Epub ahead of print.
- Kang YJ, Kim H, Lee J, Park Y, Kim JH. Effect of airborne particle abrasion treatment of two types of 3D-printing resin materials for permanent restoration materials on flexural strength. *Dent Mater* 2023;39:648–658.
- Çakmak G, Herren KV, Donmez MB, Kahveci Ç, Schimmel M, Yılmaz B. Effect of coffee thermocycling on the surface roughness and stainability of nanographene-reinforced polymethyl methacrylate used for fixed definitive prostheses. *J Prosthet Dent* 2023;129:507.e501–e506.
- Di Carlo S, De Angelis F, Brauner E, et al. Flexural strength and elastic modulus evaluation of structures made by conventional PMMA and PMMA reinforced with graphene. *Eur Rev Med Pharmacol Sci* 2020;24:5201–5208.
- The Graphenano website. [https://www.graphenanodental.com/descargas-documentos/diptico-gcam\\_en.pdf](https://www.graphenanodental.com/descargas-documentos/diptico-gcam_en.pdf). Accessed September 22, 2023.
- Hernández J, Mora K, Boquete-Castro A, Kina S. The effect of thermocycling on surface microhardness of PMMA doped with graphene: An experimental in vitro study. *J Clin Dent Res* 2020;17:152–161.
- Çakmak G, Donmez MB, Akay C, Abou-Ayash S, Schimmel M, Yılmaz B. Effect of thermal cycling on the flexural strength and hardness of new-generation denture base materials. *J Prosthodont* 2023;32:81–86.
- Arif R, Yılmaz B, Johnston WM. In vitro color stainability and relative translucency of CAD-CAM restorative materials used for laminate veneers and complete crowns. *J Prosthet Dent* 2019;122:160–166.
- Çakmak G, Donmez MB, Kashkari A, Johnston WM, Yılmaz B. Effect of thickness, cement shade, and coffee thermocycling on the optical properties of zirconia reinforced lithium silicate ceramic. *J Esthet Restor Dent* 2021;33:1132–1138.
- Donmez MB, Olcay EO, Demirel M. Load-to-failure resistance and optical characteristics of nano-lithium disilicate ceramic after different aging processes. *Materials (Basel)* 2022;15:4011.
- Acar O, Yılmaz B, Altintas SH, Chandrasekaran I, Johnston WM. Color stainability of CAD/CAM and nanocomposite resin materials. *J Prosthet Dent* 2016;115:71–75.
- Alp G, Subasi MG, Johnston WM, Yılmaz B. Effect of surface treatments and coffee thermocycling on the color and translucency of CAD-CAM monolithic glass-ceramic. *J Prosthet Dent* 2018;120:263–268.
- Zimmermann M, Ender A, Attin T, Mehl A. Fracture load of three-unit full-contour fixed dental prostheses fabricated with subtractive and additive CAD/CAM technology. *Clin Oral Investig* 2020;24:1035–1042.
- Zimmermann M, Ender A, Egli G, Özcan M, Mehl A. Fracture load of CAD/CAM-fabricated and 3D-printed composite crowns as a function of material thickness. *Clin Oral Investig* 2019;23:2777–2784.
- Corbani K, Hardan L, Eid R, et al. Fracture resistance of three-unit fixed dental prostheses fabricated with milled and 3D printed composite-based materials. *J Contemp Dent Pract* 2021;22:985–990.
- Corbani K, Hardan L, Skienhe H, Özcan M, Alharbi N, Salameh Z. Effect of material thickness on the fracture resistance and failure pattern of 3D-printed composite crowns. *Int J Comput Dent* 2020;23:225–233.
- Punset M, Brizuela A, Pérez-Pevida E, Herrero-Climent M, Manero JM, Gil J. Mechanical characterization of dental prostheses manufactured with PMMA-graphene composites. *Materials (Basel)* 2022;15:5391.
- Ionescu AC, Brambilla E, Pires PM, et al. Physical-chemical and microbiological performances of graphene-doped PMMA for CAD/CAM applications before and after accelerated aging protocols. *Dent Mater* 2022;38:1470–1481.
- Agarwalla SV, Malhotra R, Rosa V. Translucency, hardness and strength parameters of PMMA resin containing graphene-like material for CAD/CAM restorations. *J Mech Behav Biomed Mater* 2019;100:103388.
- Ciocan LT, Ghitman J, Vasilescu VG, Iovu H. Mechanical properties of polymer-based blanks for machined dental restorations. *Materials (Basel)* 2021;14:7293.
- Vichi A, Balestra D, Scotti N, Louca C, Paolone G. Translucency of CAD/CAM and 3D printable composite materials for permanent dental restorations. *Polymers (Basel)* 2023;15:1443.
- Espinar C, Bona AD, Pérez MM, Tejada-Casado M, Pulgar R. The influence of printing angle on color and translucency of 3D printed resins for dental restorations. *Dent Mater* 2023;39:410–417.
- Paravina RD, Pérez MM, Ghinea R. Acceptability and perceptibility thresholds in dentistry: A comprehensive review of clinical and research applications. *J Esthet Restor Dent* 2019;31:103–112.
- Salas M, Lucena C, Herrera LJ, Yebra A, Della Bona A, Pérez MM. Translucency thresholds for dental materials. *Dent Mater* 2018;34:1168–1174.
- The Crowntec Instructions for use. [https://nextdent.com/downloads/IFU\\_GA\\_Saremco\\_Print\\_CROWNTEC\\_EN\\_USA\\_02-2022\\_unfreiCHE.pdf](https://nextdent.com/downloads/IFU_GA_Saremco_Print_CROWNTEC_EN_USA_02-2022_unfreiCHE.pdf). Accessed September 22, 2023.
- The Tera Harz TC-80DP Technical data sheet. <https://exhibitorsearch.messefrankfurt.com/images/original/userdata/bata/212522/5d6f23fdc67d1.pdf>. Accessed September 22, 2023.
- The ODS website. <https://odsresin.co.kr/Product/cb-permanent-a1/?lang=en>. Accessed September 22, 2023.
- Choi Y, Yoon J, Kim J, Lee C, Oh J, Cho N. Development of bisphenol-A-glycidyl-methacrylate- and trimethylolpropane-triacrylate-based stereolithography 3D printing materials. *Polymers (Basel)* 2022;14:5198.